

# MONITORING OF OCEAN CURRENT PERTURBATIONS USING ACOUSTIC PHASE VARIATIONS

ADAM ZIELINSKI, MAREK BUTOWSKI, PAUL KRAEUTNER

Department of Electrical and Computer Engineering,  
University of Victoria,  
Victoria, B.C. V8W 3P6 Canada  
*Adam@uvic.ca*

*In this paper, we review an acoustic method for measuring both average ocean current speed and sound speed along an acoustic path. The method requires two or more stations on the sea floor, synchronized through a connecting underwater electric cable, that can transmit and receive an acoustic signal and The method is based on reciprocal acoustic transmissions to determine time of flight in both the forward and reverse directions. A specific implementation of this method is proposed. We also consider a novel method for monitoring ocean current perturbations through acoustic phase measurements. In simplest form, a continuous sinusoidal signal is transmitted from one station to a second station. Any variations in ocean current speed will introduce a phase shift in the received signal proportional to the time derivative of the current speed. This effect has been demonstrated through ultrasonic in-air experiments. Finally, the two methods are combined into a single system that continuously measures small-scale ocean current velocity changes.*

## INTRODUCTION

Ocean currents are the movement of seawater. This movement is composed of a bulk seawater current that changes slowly with time, possibly accompanied by quickly varying perturbations in the flow. For example, the Gulf Stream current speed in the Florida Straits exceeds 0.5 m/s near the sea floor, and may reach 2.5 m/s at the surface [1]. Ocean currents are of particular interest in the study of climate change, nutrient distribution, sediment transportation, and coastal erosion.

The methods of ocean current measurement fall into four main categories: mechanical, electromagnetic, acoustic time-of-flight, and acoustic Doppler. Mechanical current meters rely on seawater moving a rotor; the speed of rotation translates into a current speed. Although such units are inexpensive, drifting seaweed and other objects may inhibit their

mechanical moving parts. Electromagnetic current meters rely on the fact that seawater is electrically conductive. The movement of seawater through an alternating magnetic field induces an electric current across two electrodes, which may be measured to determine the seawater flow. The remaining methods rely on underwater acoustics. The time of flight method relies on measuring the forward and reciprocal travel time of an acoustic pulse. When the pulse is traveling with the current, the time of flight will decrease; the reciprocal pulse will travel against the current and the time of flight will increase. In the simplest system, two transducers are separated by a known distance and a high frequency pulse is transmitted between them. However, only the current component along the path is measured. The Doppler method relies on an acoustic echo from moving particles and bubbles in seawater. A Doppler unit sends a pulse and the received echoes from the particles and bubbles will exhibit a Doppler frequency shift. This frequency shift is related to the speed of the particles in the seawater, which is assumed identical to that of the ocean current. This method allows for the measurement of current profiles over a certain range.

## 1. AN ACOUSTIC RECIPROCAL TIME OF FLIGHT METHOD

Here, we present a method of measuring ocean current speed as well as sound speed over an acoustic path. The method is based on reciprocal transmissions [2]. In the simplest form, the system consists of two stations, A and B, located on the sea floor, separated by a known distance,  $D$ , and connected by an underwater electric cable. Each station has a transponder (or transponder array) for signal transmission and reception. The cable allows the synchronization of the two stations. Fig.1 illustrates this configuration.

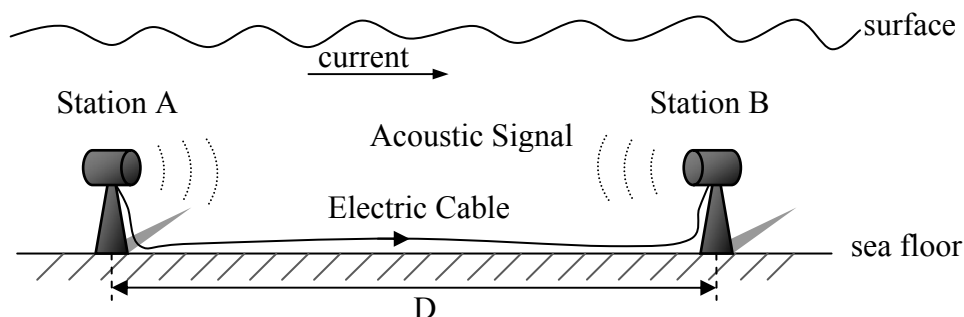


Fig.1. Two stations on sea floor

At time  $t = 0$ , a short acoustic pulse,  $s(t)$ ,

$$s(t) = A(t)e^{j2\pi f_c t}, \quad (1)$$

where  $f_c$  is the carrier frequency of the transmitted signal, with envelope,  $A(t)$ ,

$$A(t) = A_0 e^{\left(-\frac{\pi t^2}{2\tau^2}\right)} \quad (2)$$

is transmitted from A to B simultaneously with an electric synchronization pulse sent over the cable. The envelope chosen is Gaussian, such that the time-bandwidth product is minimal

[3]. The duration,  $\tau$ , of the pulse is defined as the length of a rectangular pulse of amplitude  $A_0$  with equivalent energy. To simplify the analysis, we assume that the medium is uniform, with no noise, and with no multipaths. Under these assumptions, the normalized received signal,  $\hat{s}(t)$ , is a replica of the transmitted signal delayed by the travel time from A to B,  $\tau_{AB}$ ; that is,

$$\hat{s}(t) = s(t - \tau_{AB}), \quad (3)$$

as illustrated in Fig.2.

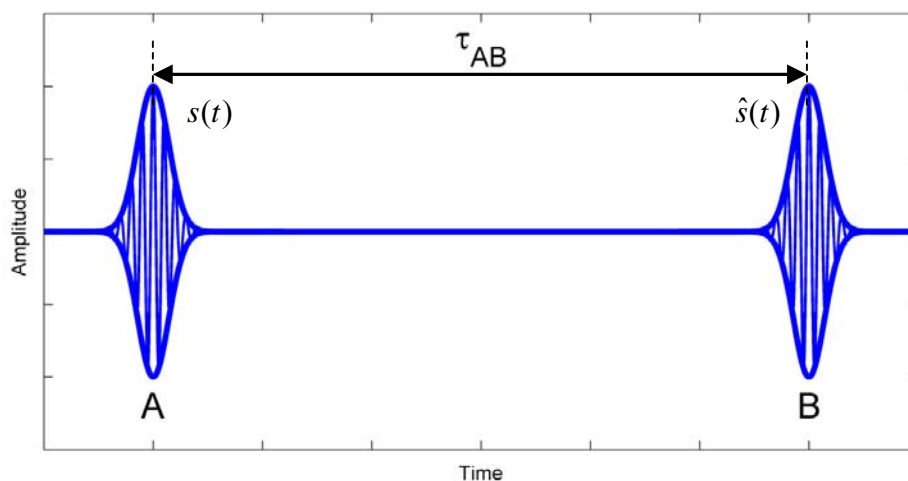


Fig.2. Transmitted and received pulse

Triggered by the electric synchronization pulse, Station B simultaneously transmits the same signal to Station A, in the reciprocal direction. Upon receiving the acoustic signal, both stations calculate the corresponding travel times,  $\tau_{AB}$  and  $\tau_{BA}$ ; and this information is shared via the electric cable. One or both of the stations then compute the average speed of sound,  $c$ , over the acoustic path,

$$c = \frac{2D}{\tau_{AB} + \tau_{BA}}, \quad (4)$$

and the average ocean current speed,  $v_{AB}$ , over the acoustic path,

$$v_{AB} = \frac{D}{2} \left( \frac{1}{\tau_{AB}} - \frac{1}{\tau_{BA}} \right). \quad (5)$$

The process repeats periodically to monitor changes in average ocean current and sound speed over the path. The delays,  $\tau_{AB}$  (and  $\tau_{BA}$ ), can be determined by numerous methods. Two such methods are match filtering and envelope detection.

The optimal method in the presence of noise is match filtering [4]. Match filtering involves a filter with output,

$$y(t) = s(t) * \hat{s}(t), \quad (5)$$

and the estimated delay,  $\hat{\tau}_{AB}$ , is determined by:

$$\hat{\tau}_{AB} = \arg \max_t [y(t)] \approx \tau_{AB} . \quad (5)$$

The other method, envelope detection, is effective when no noise is present and involves envelope,  $\hat{e}(t)$ , extraction; that is determined by,

$$\hat{e}(t) = \text{envelope}[\hat{s}(t)] , \quad (5)$$

And the estimated delay,  $\hat{\tau}_{AB}$ , is:

$$\hat{\tau}_{AB} = \arg \max_t [\hat{e}(t)] \approx \tau_{AB} \quad (5)$$

For simplicity, we will use envelope detection.

The envelope can be extracted by use of a number of methods. One method involves the in-phase,  $\hat{s}_I(t)$ , and quadrature,  $\hat{s}_Q(t)$ , components of a signal that is:

$$\hat{e}(t) = \text{envelope}[\hat{s}(t)] = |\hat{s}_I(t) + j\hat{s}_Q(t)| . \quad (5)$$

The quadrature components can be conveniently obtained through quadrature sampling [5]. In this paper, we will employ a constant sampling period,  $T_s=1/(4f_c)$ . The sampled signal,  $\hat{s}[n] = \hat{s}(nT_s)$ , is then multiplied by  $\cos(n\pi/2)$  and  $\sin(n\pi/2)$ , and low-pass filtered to generate the in-phase and quadrature samples,  $\hat{s}_I[n]$  and  $\hat{s}_Q[n]$ . Conveniently for ease of implementation,  $\cos(n\pi/2)$  and  $\sin(n\pi/2)$  are sequences of 1,0,-1,0,... and 0,1,0,-1,... respectively.

$$\begin{aligned} \tilde{s}_I[n] &= \cos\left(\frac{\pi}{2}n\right) \hat{s}(nT_s) \\ \tilde{s}_Q[n] &= \sin\left(\frac{\pi}{2}n\right) \hat{s}(nT_s) \\ \hat{s}_I[n] &= H_{LP} \{ \tilde{s}_I[n] \} \\ \hat{s}_Q[n] &= H_{LP} \{ \tilde{s}_Q[n] \} \end{aligned} \quad (5)$$

$H_{LP} \{ \dots \}$  is a low-pass filter with bandwidth less than or equal to  $f_c$  and greater than half the signal bandwidth B. Fig. 3 illustrates this method.

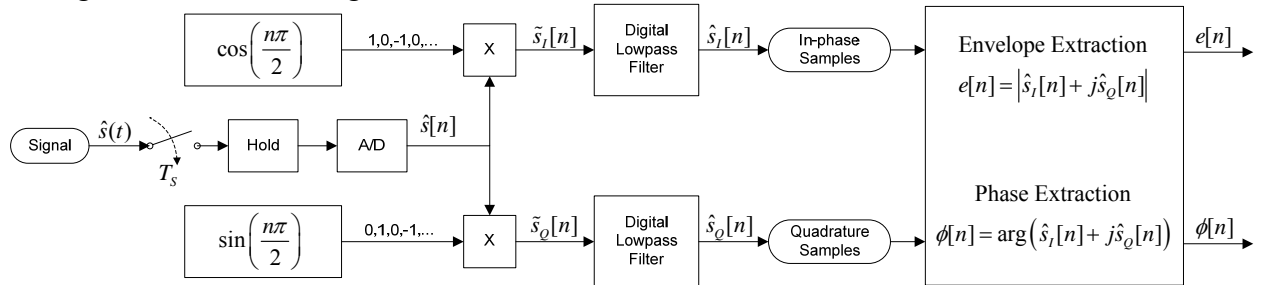


Fig.3. Quadrature sampling and envelope extraction

The block diagram resembles a conventional analog quadrature detector; however, it is implemented digitally. For a narrow band system and high resolution A/D converter, the low-pass filter is redundant and can be replaced by a decimator that rejects samples multiplied by zero; however, for broadband signals with bandwidth,  $B$ , the filter is needed to reject high frequency components above  $B/2$ . This filter also reduces error due to quantization noise [6].

The signal envelope is extracted from the in-phase and quadrature samples as per (5). The sampled phase,  $\phi[n]$ , may be extracted from the in-phase and quadrature components, as

$$\phi[n] = \arg(\hat{s}_I[n] + j\hat{s}_Q[n]). \quad (5)$$

The time at which the envelope reaches its maximum is taken as the estimated arrival time,  $\hat{\tau}_{AB}$ , for the pulse as given by (5). From the forward and reciprocal travel times, the average ocean current speed and sound speed over the acoustic path are calculated as per (4) and (5). The entire procedure described is illustrated in Fig.4.

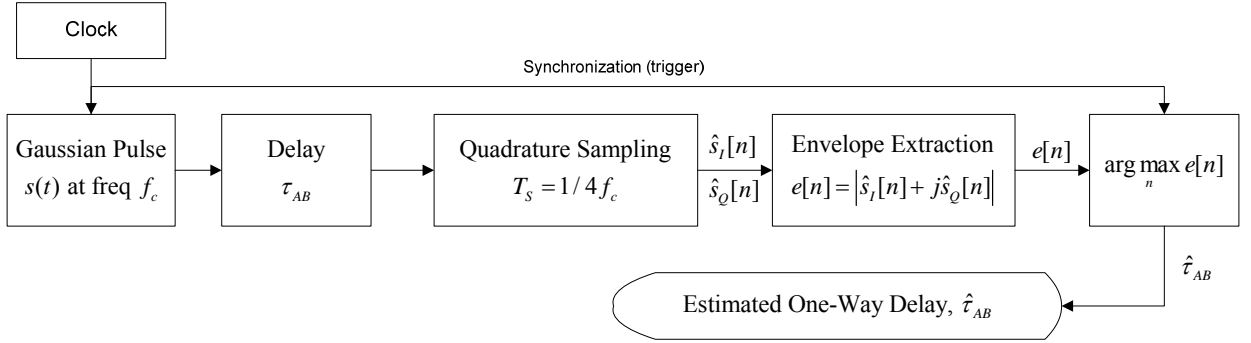


Fig.4. Simulation of delay estimation

As a specific example, we simulated the described procedure with station separation  $D = 1000$  m, and Gaussian pulse with carrier frequency  $f_c = 25$  kHz. This pulse was transmitted from station A and delayed by the travel time  $\tau_{AB}$ . The received signal was then quadrature sampled at station B, and its envelope was extracted to estimate  $\tau_{AB}$ . The simulated waveforms are shown in Fig.5.

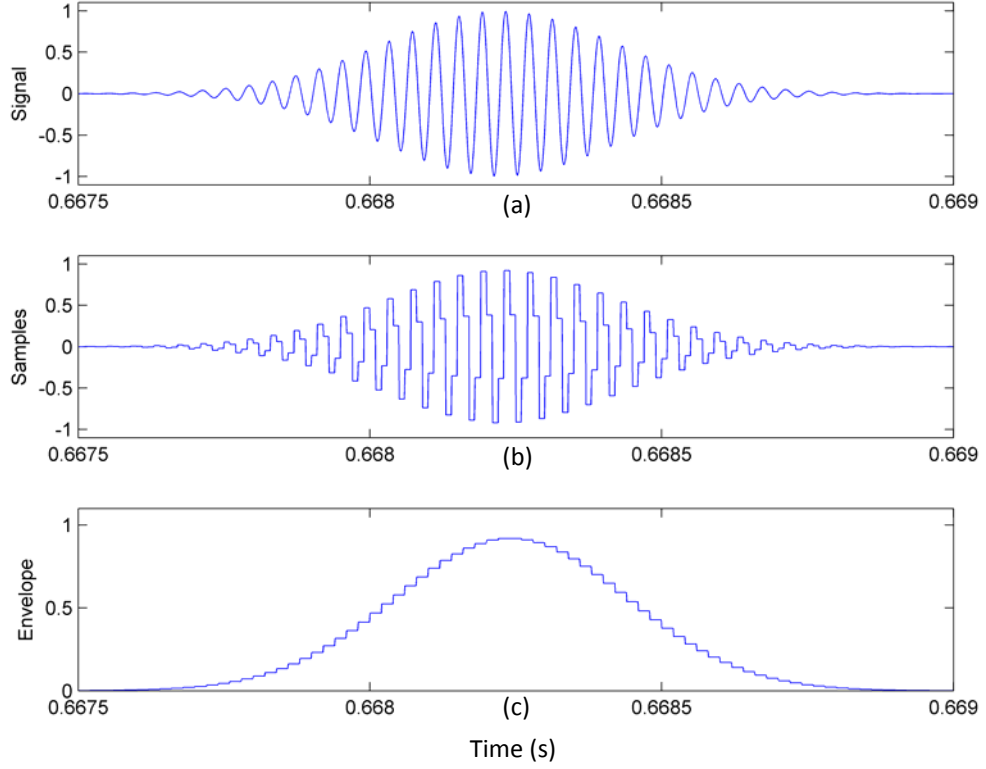


Fig.5 Simulation waveforms: (a) received signal, (b) sampled signal, and (c) extracted envelope

From these results, we determined  $\tau_{AB}$  to within  $\pm T_s$  of the actual value. To improve the resolution, the envelope can be interpolated between samples [7].

## 2. A METHOD TO MEASURE OCEAN CURRENT PERTURBATIONS

A similar system configuration will enable the measurement of small fluctuations, or perturbations, in the ocean current speed. Instead of transmitting a pulse as per (1) and (2), consider the case where station A transmits a continuous signal,  $s(t)$ :

$$s(t) = e^{j\omega_0 t} . \quad (6)$$

Again, the travel time from A to B causes the received signal at B,  $\hat{s}(t)$ , to be delayed by  $\tau_{AB}$ :

$$\hat{s}(t) = s(t - \tau_{AB}) = e^{j\omega_0(t - \tau_{AB})} = e^{j\omega_0 t} e^{-j\omega_0 \tau_{AB}} , \quad (7)$$

where

$$\tau_{AB} = \frac{D}{C + v_{AB}} , \quad (8)$$

$D$  is the distance between stations, and  $c$  is the speed of sound. Both  $D$  and  $c$  are known since  $D$  is predetermined and  $c$  is measured via reciprocal transmission (4) and are assumed to be constant over a finite travel times,  $\tau_{AB}$  and  $\tau_{BA}$ .

The delay causes a phase shift,  $\phi_{AB}$ , in the received signal,  $\hat{s}(t)$ , such that

$$\phi_{AB} = \omega_0 \tau_{AB} = \omega_0 \left( \frac{D}{c + v_{AB}} \right). \quad (9)$$

Any changes in the ocean current speed,  $v_{AB}$ , with time will cause the phase to change, so that

$$\phi_{AB}(t) = \frac{\omega_0 D}{c + v_{AB}(t)}. \quad (9)$$

Multiplying the numerator and denominator of (9) by  $[c - v_{AB}(t)]$  and assuming  $c^2 \gg v_{AB}^2$ , we obtain:

$$\phi_{AB}(t) \approx \frac{\omega_0 D}{c} - \frac{\omega_0 D}{c^2} v_{AB}(t). \quad (9)$$

Because of phase ambiguity, we will concern ourselves only with phase variations,  $\Delta\phi_{AB}(t)$ , caused by current perturbations,  $\Delta v_{AB}(t)$ ; that is, where

$$\Delta\phi_{AB}(t) = \frac{-\omega_0 D}{c^2} \Delta v_{AB}(t) \quad (10)$$

from which

$$\Delta v_{AB}(t) = \frac{-c^2}{\omega_0 D} \Delta\phi_{AB}(t). \quad (10)$$

Over time, the observed phase may flip by  $2\pi$  and needs to be unwrapped. The unwrapped phase will reflect both the perturbations and general trend in the ocean current speed.

A simulation was conducted using the same scenario as for reciprocal transmission, but now with both slowly and quickly varying current fluctuations. The current,  $v_{AB}(t)$ , was modeled by a low frequency signal,  $v_{dc}(t)$ , representing the slowly varying component of the current speed and a superimposed higher frequency signal,  $v_{ac}(t)$ , representing current perturbations. That is,

$$v_{AB}(t) = v_{dc}(t) + v_{ac}(t), \quad (11)$$

as shown in Fig.6a. This signal was used in the simulation to modulate the phase. The recovered phase is shown in Fig.6b and Fig.6c.

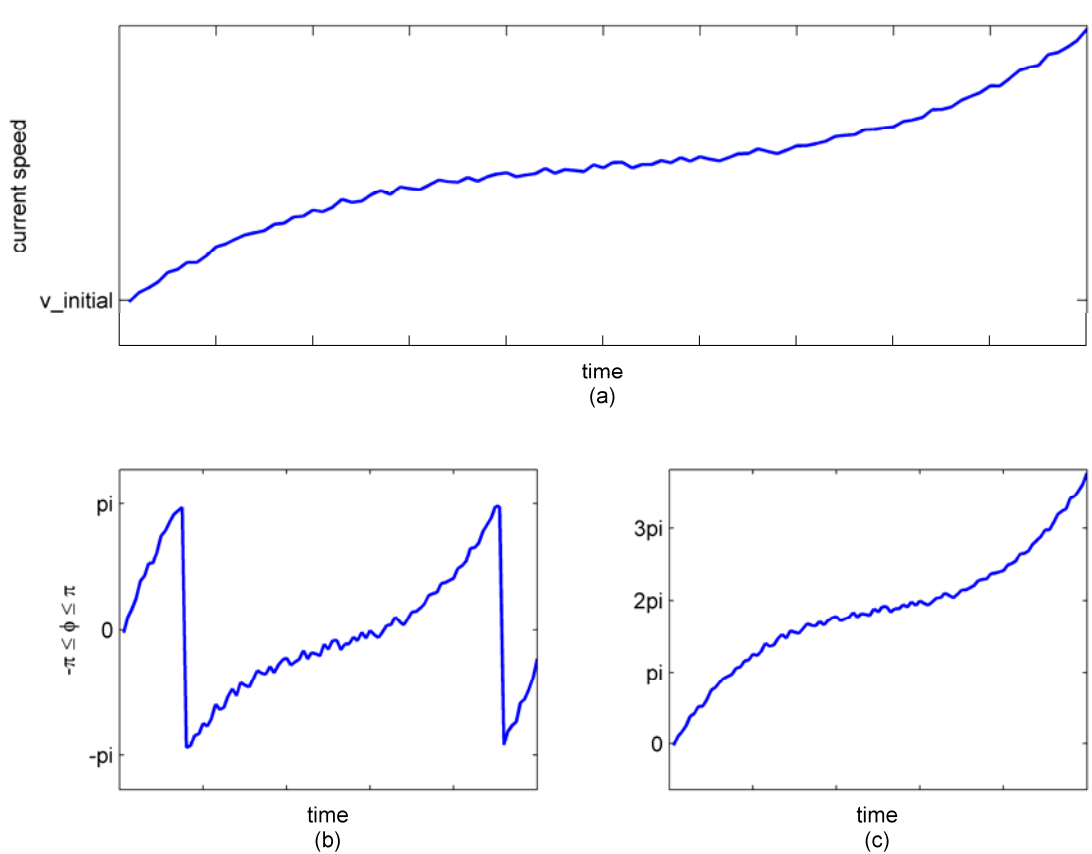


Fig.6. (a) Modeled ocean current, (b) recovered phase, and (c) unwrapped phase proportional to the current

The separation of  $v_{dc}(t)$  and  $v_{ac}(t)$  can be implemented by trend extraction. Numerous methods of trend extraction are available; a recently developed method utilizes wavelets. The basis function is chosen depending on the trend model [8]. In our simulation, the discrete Meyer wavelet gave good results, as shown in Fig.7. The initial current velocity,  $v_{initial}$ , is established through reciprocal transmission as described in Section 2.



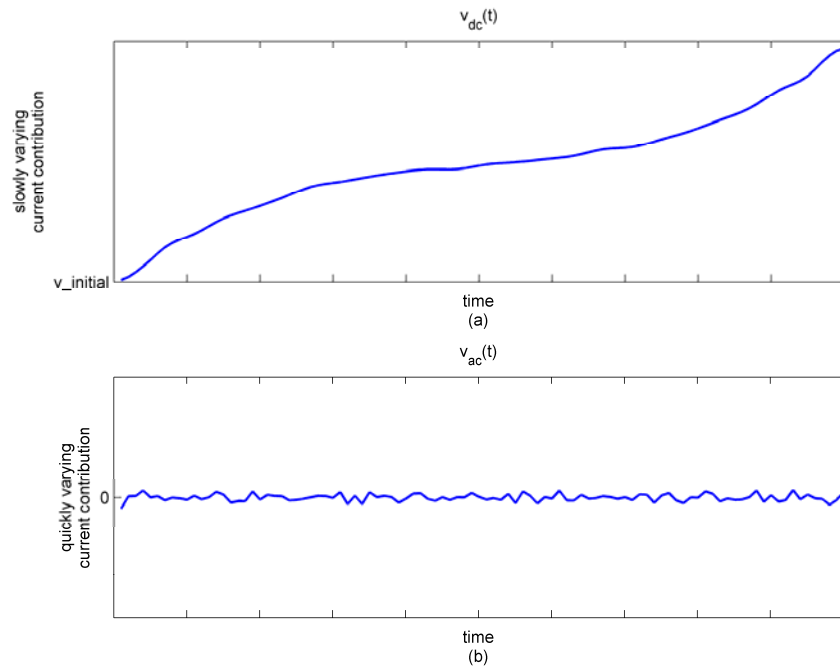


Fig.7. (a) Slowly and (b) quickly varying ocean current speed components extracted using Meyer wavelet processing

### 3. ULTRASONIC MEASUREMENT OF AIRFLOW

To demonstrate the measurement of current by acoustic phase monitoring, we conducted in-air experiments using ultrasonic transmission. The objective of those experiments was to relate phase variations to air flow speed. We used a Kobitone 400ST16 ultrasonic transmitter to transmit a continuous sinusoidal wave at a carrier frequency of 40 kHz. Two ultrasonic receivers,  $R_1$  and  $R_2$  (microphones), both Kobitone 400SR12 units, were placed in line with the transmitter and separated by a distance of  $D = 10.4$  cm as shown in Fig.8. Both receivers faced towards the transmitter and all three were placed inside a plastic tube. A fan blew air through the tube and an anemometer positioned at the end of the tube measured the air flow speed. Finally, a function generator produced the 40 kHz sinusoidal wave for the transmitter and the phase difference between the two receivers was measured by the phase detector.

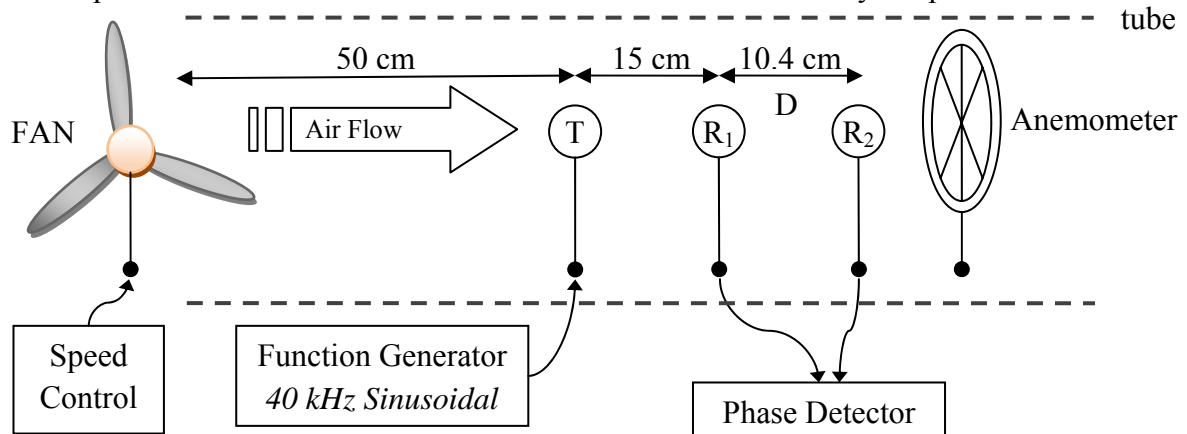


Fig.8. In-air experimental setup

With zero air flow, the initial phase,  $\phi_0$ , of the received signal at  $R_2$  was measured with reference to the signal at  $R_1$ . The fan was turned on to produce a certain airflow speed as measured by anemometer, and the phase,  $\phi_1$ , at  $R_2$  was measured again. The phase difference,  $\Delta\phi = \phi_1 - \phi_0$ , corresponds to the change in airflow speed. This procedure was repeated for three different airflow speeds.

For the first speed of 4.7 m/s, the expected phase change was  $\Delta\phi = 1.04$  radians or 60 degrees; that is,

$$\Delta\phi = \frac{2\pi}{343^2} \frac{40000 \cdot 0.104}{1} (4.7 - 0) = 1.04 \text{ rad} = 60^\circ, \quad (12)$$

where it was assumed that the sound velocity in the air,  $c = 343$  m/s. The measured phase change was 1.06 radians or 60.5 degrees. The acoustically measured speed change was, therefore,  $v_{AB} = 4.75$  m/s as given by (10). This is within the  $\pm 0.1$  m/s resolution of the anemometer used as the reference. Experimental results for the other air speeds,  $v_{AB}$ , and two other distances,  $D$ , are shown in Tab.1.

Tab.1. Ultrasonic in-air experiment data

<b>Receiver Separation D [m]</b>	<b>Measured <math>\Delta\phi_{AB}</math> [rad]</b>	<b>Anemometer <math>v_{AB}</math> [m/s]</b>	<b>Acoustic <math>v_{AB}</math> [m/s]</b>	<b>Error [m/s]</b>	<b>Error [%]</b>
0.104	1.056	4.7	4.75	+ 0.05	+ 1.1
0.104	1.181	5.3	5.32	+ 0.02	+ 0.4
0.104	1.257	5.8	5.66	+ 0.14	+ 2.4
0.188	1.784	4.3	4.44	+ 0.14	+ 3.3
0.188	2.061	5.0	5.13	+ 0.13	+ 2.6
0.188	2.337	5.5	5.82	+ 0.32	+ 5.8
0.255	2.463	4.3	4.52	+ 0.22	+ 5.1
0.255	2.714	4.8	4.98	+ 0.18	+ 3.8
0.255	3.041	5.4	5.58	+ 0.18	+ 3.3

#### 4. A PROPOSED SYSTEM AND PRACTICAL CONSIDERATIONS

It is of interest to combine reciprocal transmission and continuous phase monitoring into one system. Reciprocal transmission establishes the speed of sound over the acoustic path and the ocean current speed at a low sampling rate, while continuous phase monitoring provides measurements of changes in the ocean current speed at a high sampling rate. The two readings can be combined into one high-rate measurement of ocean current speed, from which the general trend and perturbations of the ocean current speed may be extracted. This concept is illustrated in Fig.9.

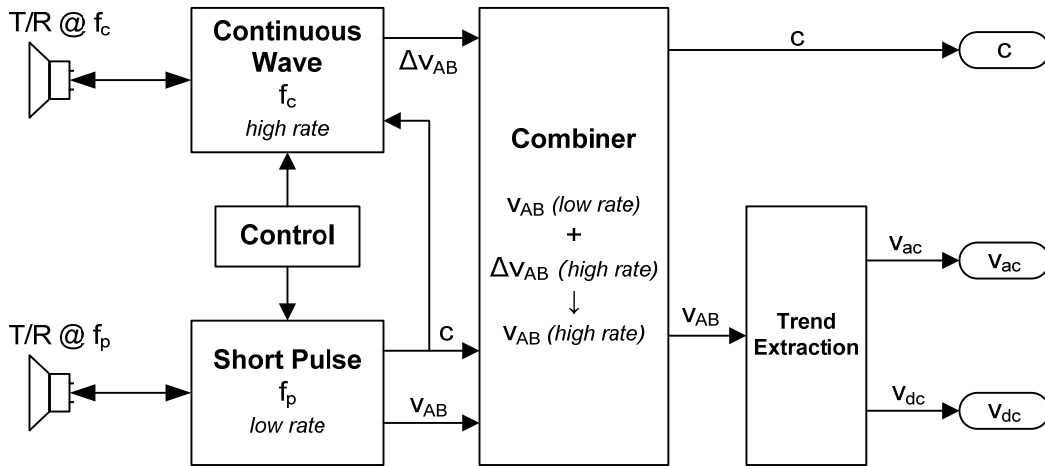


Fig.9. A practical system using both reciprocal transmission and continuous phase monitoring

Each station has two transmitters and receivers operating at two different frequencies,  $f_c$  and  $f_p$ , to allow for parallel operation. The reciprocal transmission is used periodically to establish sound speed and ocean current speed along the acoustic path as described in Section 2. Continuous phase monitoring provides a high rate measurement of the change in ocean current speed along the path as described in Section 3. The two tasks generate data at two different rates that may be combined. The combiner generates a single high rate ocean current speed reading. This reading is split through trend extraction into a slowly varying trend and quickly varying perturbation as described at the end of Section 3.

The feasibility of this system is dependent on a number of previously made assumptions. The distance between the two stations is fixed and must be determined. A GPS/USBL positioning system, such as the IXSEA GAPS, can determine the location of each station. This unit has an accuracy of 0.2% of the slant range [9]. The position error is minimized when the GAPS unit is directly over the station. In our scenario, we assumed the two stations were positioned at a depth of 300 m and were separated by 1000 m. Therefore, the location of each station could be determined to  $\pm 0.6$  m with respect to the GAPS unit.

A critical design parameter is the signal to noise ratio, S/N, of the system. Each station is equipped with a horizontally nondirectional and vertically narrow-beam transducer or array. Let us assume that the continuous wave (CW) system operates at frequency 17.5 kHz with vertical beamwidth of  $\pm 10^\circ$ . Let a system bandwidth  $B = 1$  kHz; the ambient ocean noise at 17.5 kHz in a calm sea is 67.7 dB re  $1 \mu\text{Pa}$ . With these parameters and transmitted acoustic power of 1 watt, the S/N ratio at the receiver exceeds 60 dB.

The system will also be affected by multipaths. The surface and the sea bottom cause the two main multipaths. The sea bottom multipath will be constant with time and will not affect continuous phase monitoring. The surface multipath will vary with tides and surface conditions; however, the directionality of the transducers will reduce its effect. In our scenario, the surface multipath arrives at the transducer at incident angle of  $31^\circ$ . This provided 38 dB of suppression on the transmit side and another 38 dB on the receive side.

The practical system described here uses an underwater electrical cable to synchronize the stations. A plausible modification is to use buoys equipped with GPS for synchronization and Iridium satellites for data transfer. These buoys are connected to the stations by electric cables. With GPS time, the two stations can be synchronized to within  $\pm 25$  ns [10].

## 5. FUTURE WORK

The next step is to build two demonstration stations for ocean current measurements. Each station must be capable of transmitting arbitrary waveforms to allow for the evaluation of both continuous and pulsed signals of varying type; as well, each station must be able to receive a wide band signal. These stations will be capable of demonstrating the simple concepts described in this paper, but should also be capable of testing advanced concepts, such as coded continuous wave transmissions.

A possible extension of the system is to use more than two stations. Three stations would permit the measurement of currents in a plane, assuming current uniformity [11]. A mesh of stations would allow the measurement of non-uniform ocean currents and ocean eddies.

A final proposed system change is to extract both the time of arrival and phase from a coded acoustic wave.

## REFERENCES

- [1] Knauss, J., *Introduction to Physical Oceanography*. Upper Saddle River, NJ: Prentice Hall, 1997, pp. 138.
- [2] Zheng, H., Gohda, N., Noguchi, H., Ito, T., Yamaoka, H., Tamura, T., Takasugi, Y., Kaneko, A., "Reciprocal Sound Transmission Experiment for Current Measurement in the Seto Inland Sea, Japan." *Journal of Oceanography*, vol. 53, 1997, pp. 117-127.
- [3] de Coulon, F., *Signal Theory and Processing*. Dedham, MA: Artech House, 1986, p. 249.
- [4] Carlson, A., *Communication Systems*. 2nd ed. New York: McGraw-Hill, 1975, pp. 156-158.
- [5] Liu, H., Ghafoor, A., Stockmann, P.H., "A New Quadrature Sampling and Processing Approach." *IEEE Transactions on Aerospace and Electronic Systems*, vol.25, no.5, pp.733-748, Sep 1989.
- [6] Xiong, X., Zielinski, A. "An Adaptive Algorithm for Amplitude and Phase Measurements Based on Multiple Sampling." *Oceans 2007 Conference*, Vancouver, September 29 - October 4, 2007, 6 pages, paper 070426-014 (on CD).
- [7] Weisstein, E., "Nonlinear Least Squares Fitting." *MathWorld: A Wolfram Web Resource*. <http://mathworld.wolfram.com/NonlinearLeastSquaresFitting.html>.
- [8] Alexandrov, T., Bianconcini, S., Dagum, E.B., Maass, P., McElroy, T., "A Review of Some Modern Approaches to the Problem of Trend Extraction." *Statistical Research Division U.S. Census Bureau*, March 2008.
- [9] IXSEA, "GAPS – Portable, Calibration Free USBL." <http://www.ixsea.com/pdf/2008-01-ps-gap.pdf>.
- [10] Spectracom, "Epsilon Clock Model EC1S." [http://www.spectracomcorp.com/Portals/0/products/pdf/Epsilon\\_Clock\\_Model\\_EC1S.pdf](http://www.spectracomcorp.com/Portals/0/products/pdf/Epsilon_Clock_Model_EC1S.pdf).
- [11] Zielinski, A., Zhou, L., Butowski, M., "Ocean Average Current Measurement Using Acoustic Phase Monitoring." *Hydroacoustics, Vol. 11*, Gdansk, May 2008, pp. 459-466.